Application Note

Immunology

Automated Analysis of Neutrophil NETosis Activity

Using the Agilent BioTek Lionheart FX to image and analyze stimulated dHL-60 cells

Author

Paul Held, PhD
Agilent Technologies, Inc.

Abstract

Neutrophils play a key role in the body's defense against infections, as part of the innate immune system they employ multiple strategies to degrade and kill microbes including the release of neutrophil extracellular traps (NETs). NETs are a web-like structure composed of antimicrobial proteins and DNA that are released during a distinct form of programmed neutrophil cell death known as NETosis. In general, NETs allow neutrophils to kill extracellular pathogens while minimizing damage to the host cells, but can also result in an autoimmune response. This process *in vivo* is not well understood, and the development of *in vitro* models means to further elucidate the mechanisms and results of this phenomenon are desirable. This application note describes the use of the Agilent BioTek Lionheart FX imager to image and analyze differentiated HL-60 cells stimulated to undergo NETosis *in vitro*.

Introduction

Neutrophil extracellular traps (NETs) are networks of extracellular fibers, primarily composed of DNA from neutrophils, which bind pathogens.[1] Neutrophils, which are the most abundant white blood cell and the immune system's first-line of defense against infection, have conventionally been thought to kill invading pathogens by either engulfment of microbes or the secretion of antimicrobials.[2] In 2004, a third function, the formation of NETs, was identified by Brinkmann *et al.*[1] High-resolution scanning electron microscopy has shown that NETs consist of stretches of DNA and globular protein domains with diameters of 15 to 17 nm and 25 nm, respectively, which can aggregate into larger threads with a diameter of 50 nm.[1] Under the flow conditions present in the vasculature *in vivo*, much larger structures can form.[3]

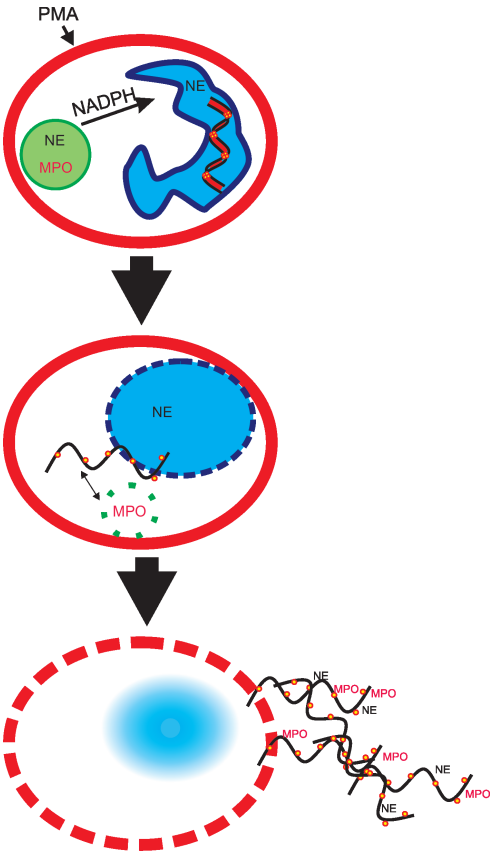

Figure 1. NETosis process.

Following PMA stimulation, NETosis is activated through NADPH oxidase stimulation. NADPH oxidase assists in the translocation of neutrophil elastase (NE) from cytosolic granules into the nucleus where it aids in chromatin breakdown via histone cleavage. Myeloperoxidase (MPO) is required for chromatin and nuclear envelope breakdown and granular mixing within the NET vacuole. Following intracellular NET formation, the neutrophil outer membrane ruptures, and the mature NET is extruded.

Immunofluorescence has shown that NETs contain proteins from several different neutrophil granule types, as well as the nucleus, but many common cytoplasmic proteins, such as actin and tubulin were lacking.[1,4] NETs provide for a high local concentration of antimicrobial components that bind, disarm, and kill microbes extracellularly and independent of phagocytic uptake. Delivery of the granule proteins into NETs may also keep potentially injurious proteins like proteases from diffusing away and inducing damage in tissue adjacent to the site of inflammation.

The complete NETosis activation pathway is still under investigation but a few key proteins have been identified. The NETosis pathway can be initiated through activation of Toll-like Receptors (TLRs), Fc receptors, and complement receptors with various ligands such as antibodies, PMA, and IL-8.[5,6] Following stimulation by PMA through activation of protein kinase C, raf–mitogen-activated protein kinase and (MEK)–extracellular signal-regulated kinase (ERK) pathways, downstream signaling results in the release of calcium from the endoplasmic reticulum. This intracellular influx of calcium in turn activates NADPH oxidase, causing the activation of protein-arginine deiminase 4 (PAD4) via reactive-oxygen species (ROS) intermediaries. PAD4 is responsible for the citrullination of histones in the neutrophil, resulting in decondensation of the chromatin. Azurophilic granule proteins such as myeloperoxidase (MPO) and neutrophil elastase (NE) enter the nucleus and further the decondensation process. Eventually the nuclear envelope ruptures and the uncondensed chromatin enters the cytoplasm where additional granule and cytoplasmic proteins are added to the early-stage NET. The end result of the process then depends on whether the suicidal or vital NETosis pathway is activated (Figure 1).[7] Suicidal NETosis, first described in 2007, demonstrated that the release of NETs resulted in neutrophil-death through a different pathway than apoptosis or necrosis.[5] In suicidal NETosis, the intracellular NET formation is followed by the rupture of the plasma membrane, releasing it into the extracellular space. Vital NETosis, on the other hand, results in the blebbing of the nucleus, producing a DNA-filled vesicle that is exocytosed leaving the plasma membrane intact. While not viable,

neutrophils can continue to phagocytose and kill microbes after vital NETosis.[6] Of note, suicidal NETosis can take hours, while vital NETosis can be completed in a matter of minutes, which suggests different functions.

This application note demonstrates an *in vitro* live cell assay to monitor NETosis activity using differentiated HL-60 cells as a model. The basis of this assay is to kinetically follow cell membrane integrity using both cell membrane permeable and impermeable nuclear stains using fluorescence microscopy. This allows for the determination of inhibitor potency of NETosis activity.

Materials and methods

Reagents

RMPI-1640 tissue culture media, fetal bovine serum (FBS), glutamine, and penicillin/streptomycin were from Life Technologies. HL-60 human promyeloblast cells were obtained from ATCC (Manassas, VA). Nuclear Red and Nuclear Green stains were obtained from Cayman Chemical (Ann Arbor, MI). DMSO and ATRA, were procured from Sigma-Aldrich (St. Louis, MO). Stimulant and inhibitor small molecule compounds, PMA, Nigericin, A23187, DPI, Go 6976, nocodazole, apocynin, ML 171, VAS 2870, and NoxA 1ds were purchased from Tocris Bioscience (Minneapolis, MN).

Cell culture

HL-60 cells were grown in RPMI-1640 plus 10% FBS supplemented with 2 mM glutamine, penicillin and streptomycin. The suspension cells were split 1:5 with fresh media every 2 to 3 days. HL-60 cells were diluted to 1 × 10^5 cells/mL and differentiated into neutrophils by exposure to 1.25% DMSO and 0.1 µM ATRA for 4 to 5 days (Figure 2).

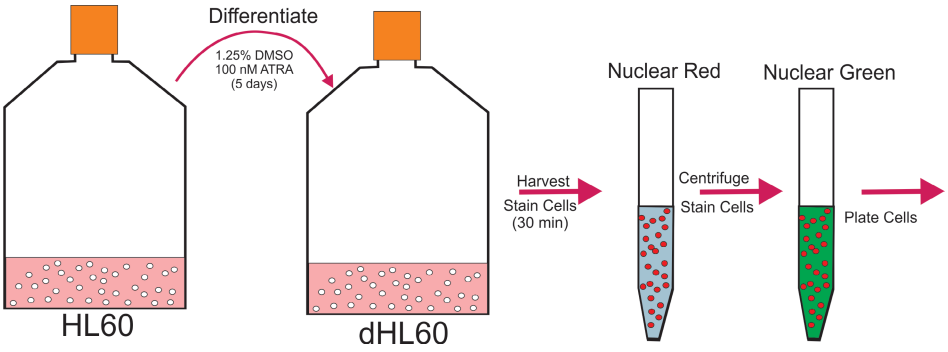

Figure 2. Differentiation of HL-60 promyelocytic leukemia cells. Cultured HL-60 cells are induced to differentiate to neutrophils by exposure to 1.25% DMSO and 100 nM ATTRA for 5 days. Differentiated HL-60 cells (dHL-60) are harvested and stained with Nuclear Red for 30 minutes at 37 °C. The cells are then pelleted, and Nuclear Green stain is added immediately before plating.

Staining

Differentiated HL-60 cells (dHL-60) were counted and 1.2 × 10^6 cells were pelleted by centrifugation in a 15 mL conical tube. Cells were resuspended in 6 mL of PBS and 6 µL of Nuclear Red stain added. Cells were incubated for 30 minutes at 37 °C, then an additional 6 mL of PBS added and the cells were again pelleted by centrifugation. Cells were resuspended in 12 mL of NETosis imaging buffer (PBS, 0.5% w/v BSA, 0.1% w/v glucose) to which 12 µL of Nuclear Green stain has been added and immediately aliquoted (100 µL, 20,000 cells/well) into the wells of a Corning (part number 3904) 96-well, black sided, clear-bottom microplate (Figure 3).

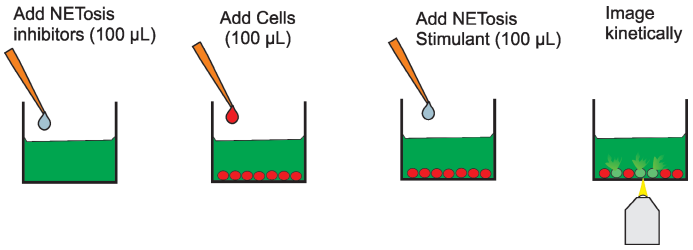

Figure 3. NETosis stimulation and inhibition assay process. Differentiated HL-60 (dHL-60) cells, prestained with Nuclear Red and Nuclear Green dyes are added to different concentrations of NETosis inhibitors before the addition of a NETosis stimulant such as PMA. After the addition of stimulant, NETosis is monitored by imaging in the GFP and CY5 channels.

Several different compounds were used to stimulate dHL-60 cells to undergo NETosis. Compound dilutions in NETosis imaging buffer were added to the wells in 100 µL at 2x of the desired concentration. Cells were then added to the wells in 100 µL and the microplate centrifuged at 200 × g for 60 seconds to seat the nonadherent cells on the bottom of the well. Imaging was initiated immediately after centrifugation.

Several potential inhibitors were studied for their ability to reduce or eliminate compound induced NETosis stimulation. Inhibitor compounds were diluted in NETosis imaging buffer and aliquoted (100 µL) into wells of a microplate at 3x the final intended concentration. dHL-60 cells (100 µL), stained as described previously, were added to the inhibitor dilutions and incubated for 15 minutes at RT, after which 100 µL of a 3x final concentration NETosis stimulate was added. The plate was centrifuged and imaged as described previously.

Imaging

Cultures were imaged using an Agilent BioTek Lionheart FX imager configured with brightfield, as well as GFP and CY5 LED cubes. The imager uses a combination of LED light sources in conjunction with bandpass filters and dichroic mirrors to provide appropriate wavelength light. Images were taken kinetically every 15 minutes for 4 hours using a 20x objective. Laser autofocus (LAF) was used to automatically focus the image for each well. A LAF reference scan was obtained using focused CY5 fluorescent images (Figure 4).

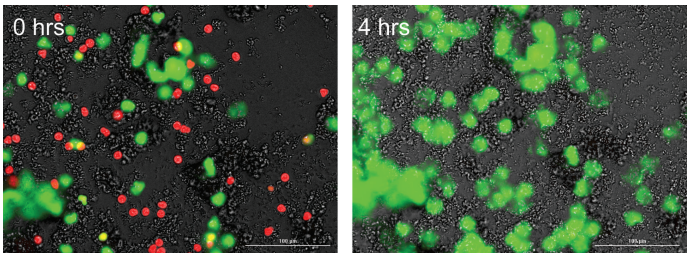

Figure 4. Cell staining. Cells were stained using a NETosis imaging assay kit (Cayman Chemical, Ann Arbor MI), which consist of a combination of Nuclear Red and Nuclear Green stains. The cell permeable red stain was used to set initial laser autofocus (LAF) parameters, while impermeable green stain was used to monitor NETosis.

Analysis

After imaging, cellular analysis identified GFP objects using a threshold value of 5,000 (Figure 5). The object masks were not split into individual objects, but were limited to greater than 10 µm in size in order to exclude debris. Holes in the mask were filled and objects along the imaging-edge were also included in the object area metric determination (Table 1).

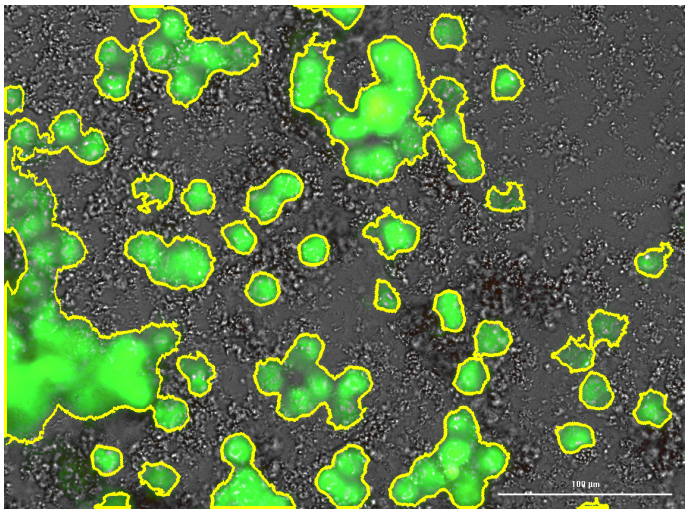

Figure 5. Object area analysis. NETs were identified using the cellular analysis data reduction option in Agilent BioTek Gen5 software. The total object area was determined for each 20x image.

Table 1. Image-capture and image-analysis parameters for NETosis.

Imaging	
Parameter	**Value**
Channel	CY5 628, 685
	GFP 469, 525
	Brightfield
Focus	Laser autofocus
Objectives	20x
Z-Stack	No
Montage	No
Offsets	
Horizontal Offset	0
Vertical Offset	0
Object Selection	
Channel	GFP 469, 535
Threshold	
Value	5,000
Background	Dark

Parameter	Value
Split Touching Obj.	No
Fill Holes in Masks	Yes
Advanced Options	
Smoothing	0
Background	5% lowest pixels
Object Size Selection	
Min	10 µm
Max	1,000 µm
Include Edge Objects	Yes
Entire Image	Yes
Object Analysis	
Metric of Interest	Object area

The total GFP object area was automatically calculated for each well at each time point and plotted using Agilent BioTek Gen5 image analysis software. The integral or area under the curve (AUC) of these plots determined automatically by Gen5 (Figure 6). The results AUCs were graphed against compound (stimulant or inhibitor) concentration using GraphPad Prism 7.

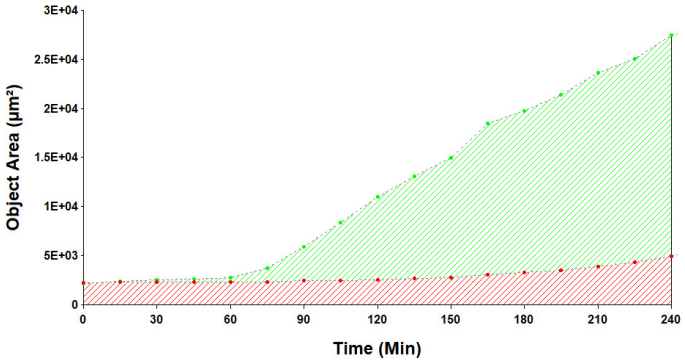

Figure 6. Integral of total green area. The total object area of green fluorescence is determined for each time point in every well of the kinetic experiments. The area under the curve (AUC) or integral of the kinetic plots for each well are automatically calculated and plotted against compound (stimulant or inhibitor) concentration depending on the experiment. The green and red striping represents the AUC for a positive and negative control, respectively.

Results and discussion

Different compounds were tested for their ability to stimulate NETosis in dHL-60 cells. By plotting the AUC of the kinetic curves as a function of compound concentration, one can ascertain the potency of various stimulators or inhibitors of NETosis. The compound phorbol 12-myristate 13-acetate (PMA) was found to be a potent stimulator of NETosis. PMA acts in a concentration dependent manner with an EC_{50} of 5 nM (Figure 7). PMA mimics diacylglycerol and binds to protein Kinase C (PKC), activating the kinase. Downstream effects include the promotion of cell growth and inflammation.[8]

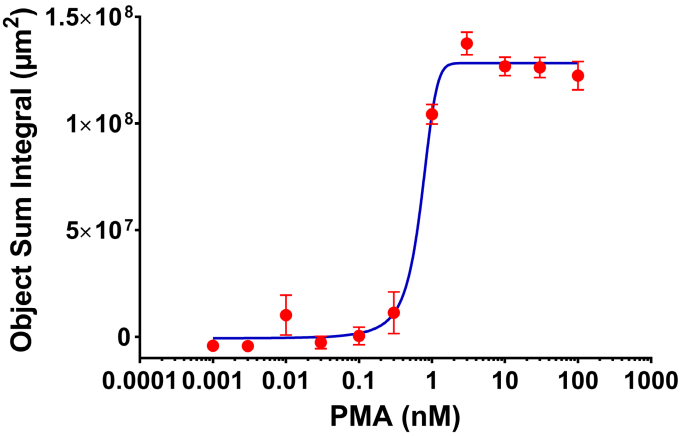

Figure 7. Effect of PMA concentration on NETosis. dHL-60 cells were treated with PMA at various concentrations in the presence of Nuclear Green stain. Analysis of kinetic images determined the total NETosis area of green fluorescence for each well as a function of time. AUC for each kinetic curve was and plotted as a function of PMA concentration. Each data point represents the mean of 8 determinations.

The ionophore compounds A23187 and Nigericin were also demonstrated to induce NETosis, as measured by GFP fluorescence, in a concentration-dependent manner. However these compounds are significantly less potent than PMA (Figure 8). A23187 is a calcium ionophore that besides directly facilitating extracellular calcium movement into the cell also activates phospholipase C-dependent mobilization of intracellular Ca^{2+} stores.[9] Nigericin is an antibiotic derived from *Streptomyces hygroscopicus* and is reported to act as a potassium ionophore, which can activate the NLRP3 inflammasome.[10]

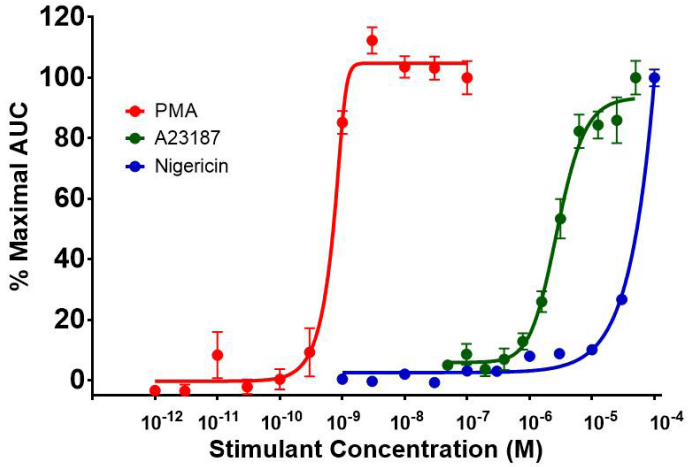

Figure 8. Comparison of the potency of different NETosis stimulant. dHL-60 cells were treated with PMA, A23187, or Nigericin at various concentrations in the presence of Nuclear Green stain. Analysis of kinetic images determined the total NETosis area of green fluorescence for each well as a function of time. AUC for each kinetic curve was calculated and plotted as a percentage of the AUC at maximum compound concentration. Each data point represents the mean of 8 determinations.

NETosis *in vivo* has been reported to act through the action of NADPH oxidase (NOX). As such, it would be expected that NOX inhibitors would ameliorate the effect of NETosis stimulants. As demonstrated in Figure 9, diphenylene iodonium (DPI) is capable of inhibiting NETosis stimulated by PMA (100 nM) in a concentration-dependent manner. Interestingly, the compound was ineffective against the ionophores A23187 or Nigericin. This suggests that these compounds act primarily though their ionophore activity rather than true stimulation of NETosis.

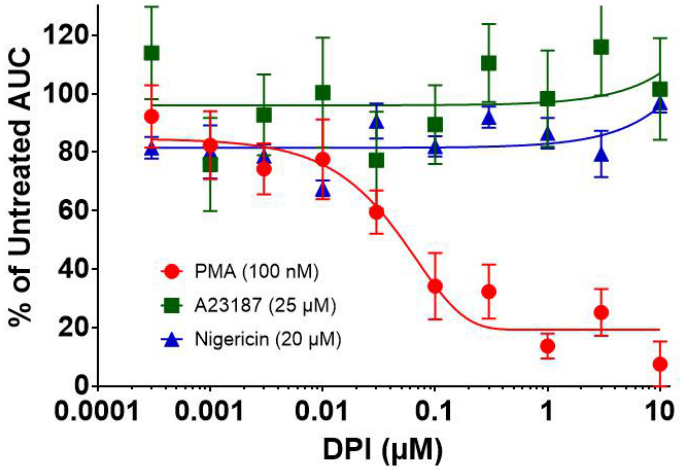

Figure 9. Inhibition of NETosis stimulation of dHL-60 cells by diphenylene iodonium (DPI). Differentiated HL-60 cells were pretreated with DPI at various concentrations prior to stimulating cells by the addition of 100 nM PMA, 25 µM A 23187, or 25 µM Nigericin in the presence of Nuclear Green stain. The integral (AUC) of the kinetic plots for total area of fluorescence for each well were calculated by Agilent BioTek Gen5 analysis software. The data was expressed as the % total AUC of untreated positive control and plotted as a function of DPI concentration. Each data point represents the mean of 8 determinations.

Several compounds were tested for their ability to inhibit the effects of PMA in regards to NETosis. As shown in Figure 10, DPI is significantly more potent and effective than the PKC inhibitor Go 6976 at negating the NETosis produced by PMA. The EC_{50} of Go 6976 is approximately 20-fold higher concentration than that observed with DPI. In addition, the effective inhibition was about half that observed with DPI. Nocodazole, which interferes with microtubule polymerization and a known cell cycle inhibitor was ineffective at preventing NETosis (Figure 9).

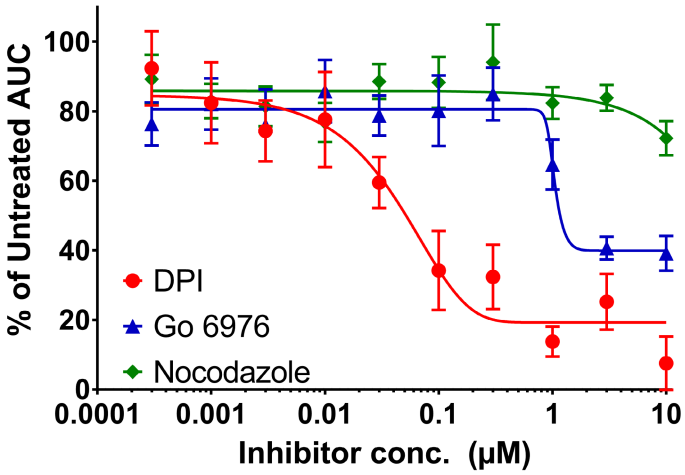

Figure 10. Effect of cellular inhibitors on PMA stimulation of dHL-60 cells. Differentiated HL-60 cells were pretreated with either DPI, Go 6976, or Nocodazole at various concentrations prior to stimulating cells by the addition of 100 nM PMA in the presence of Nuclear Green stain. The integral (AUC) of the kinetic plots for the total area of fluorescence for each well were calculated. Data was expressed as the % total AUC of untreated positive control and plotted as a function of inhibitor concentration. Each data point represents the mean of 8 determinations.

The effectiveness of the NOX inhibitor DPI at inhibiting PMA induced NETosis led us to test the efficacy of other known NOX inhibitors. Of the inhibitors tested, DPI had the greatest potency (Figure 11). Interestingly, nonspecific NOX inhibitors such as DPI, Apocynin, and VAS 2870 all had some degree of efficacy, while NOX 1 specific inhibitors had little effect (Figure 10).

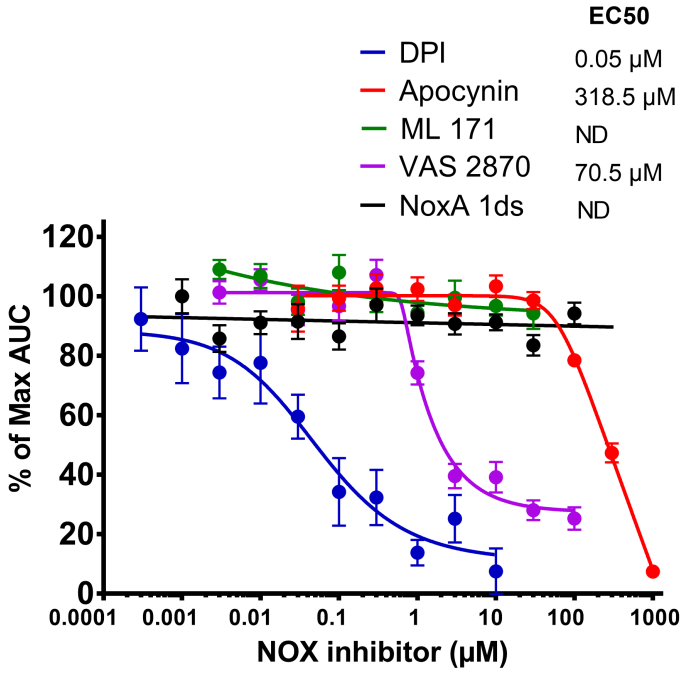

Figure 11. Effect of NADPH oxidase inhibitors on PMA stimulation of dHL-60 cells. Differentiated HL-60 cells were pretreated with either DPI, VAS 2870, Apocynin, NoxA 1ds, and ML 171 at various concentrations prior to stimulating cells by the addition of 100 nM PMA in the presence of Nuclear Green stain. The integral (AUC) of the kinetic plots for the total area of fluorescence for each well were calculated, expressed as the % total AUC of untreated positive control, and plotted as a function of inhibitor concentration. Each data point represents the mean of 8 determinations.

Conclusion

Differentiated HL-60 (dHL-60) cells were used as an *in vitro* model for human neutrophils. dHL-60 cells exhibit the same NETosis response as freshly isolated human cells and serve as a good model to better understand this phenomenon. NETosis was examined using imaging after staining with a combination of Nuclear Red and Nuclear Green (Cayman Chemical). While both stains bind nucleic acids and become fluorescent, Nuclear Red stain is a cell permeable stain that can stain live cell nuclei and Nuclear Green is impermeable and will only fluorescence when cell membranes have been disrupted. Initial imaging and focus

are accomplished using a CY5 LED cube that detects the nuclei of all cells stained with Nuclear Red. With NETosis, cell membranes become permeable to Nuclear Green dye. Entry of the dye allows an increase in green fluorescence as a result of binding to nuclear DNA. With time, the nuclear membrane breaks down and karyoplasm and cytoplasm contents mix and the nuclear contents are released. The extracellular DNA is also accessible to the Nuclear Green reagent, resulting in a greater area of green fluorescence.

The phorbol ester PMA was demonstrated to stimulate NETosis in HL-60 cells that had been differentiated into neutrophils in a dose-dependent manner. The effect could also be inhibited with NADPH oxidase inhibitors such as DPI. Ionophores such as Nigericin and A23187 were shown to have a similar effect, but could not be inhibited with DPI which suggest that their effect was not pharmacologic of NETosis, but rather the result of the ionophores allowing access of the membrane impermanent dye to the cellular nucleic acids. The NOX inhibitor data suggests, that while NADPH oxidase protein activity is required for NETosis, NOX1 is not the isoform directly responsible for this activity.

These data demonstrate that the Agilent BioTek Lionheart FX imaging microplate reader in conjunction with Agilent BioTek Gen5 data analysis software can be used to quantitate NETosis of neutrophils *in vitro*. The Lionheart FX is an ideal platform for these studies. The imager maintains physiologic temperature within the read chamber, as well as provides humidity with use of the humidity plate carrier during the kinetic imaging. Agilent BioTek Gen5 data analysis software controls the imager in regards to timing of kinetic imaging as well as automatically identifying and quantifying areas of fluorescent staining. These data are then plotted as individual well kinetic graphs and the integral (AUC) calculated. Subsequent AUC determinations are available for concentration dependent graphs.

References

1. Brinkmann, V. *et al.* Neutrophil Extracellular Traps Kill Bacteria. *Science* **2004**, *303(5663)*, 1532–1535. doi:10.1126/science.1092385. PMID 15001782.
2. Witko-Sarsat, V. *et al.* Neutrophils: molecules, functions and pathophysiological aspects. *Lab Invest*. **2000**, *80(5)*, 617–53. doi:10.1038/labinvest.3780067. PMID 10830774.
3. Clark, S. R. *et al.* Platelet Toll-Like Receptor-4 Activates Neutrophil Extracellular Traps to Ensnare Bacteria in Endotoxemic and Septic Blood. *Nature Medicine* **2007**, *13(4)*, 463–469. doi:10.1038/nm1565. PMID 17384648.
4. Urban, C. F. *et al.* Neutrophil Extracellular Traps Contain Calprotectin, a Cytosolic Protein Complex Involved in Host Defense Against Candida Albicans. *PLOS Pathogens* **2009**, *5(10)*, e1000639. PMC 2763347. doi:10.1371/journal. ppat. 1000639.
5. Fuchs, T. A. *et al.* Novel Cell Death Program Leads to Neutrophil Extracellular Traps. *The Journal of Cell Biology* **2007**, *176(2)*, 231–241. doi:10.1083/jcb.200606027. ISSN 0021-9525. PMC 2063942. PMID 17210947.
6. Yang, H. *et al.* New Insights into Neutrophil Extracellular Traps: Mechanisms of Formation and Role in Inflammation. *Frontiers in Immunology* **2016**, *7*, 302. PMID 27570525. doi:10.3389/fimmu.2016.00302. ISSN 1664-3224. PMC 4981595.
7. Jorch, S. K.; Kubes, P. An Emerging Role for Neutrophil Extracellular Traps in Noninfectious Disease. *Nature Medicine* **2017**, *23(3)*, 279–287. doi:10.1038/nm.4294. ISSN 1078-8956. PMID 28267716.
8. Moscat, J.; Diaz-Meco, M. T.; Rennert, P. NF-κB Activation by Protein Kinase C Isoforms and B-Cell Function. *EMBO Reports* January **2003**, *4(1)*, 31–36. doi:10.1038/sj.embor.embor704. PMC 1315804.
9. Dedkova, E. N., Sigova, A. A.; Zinchenko, V. P. Mechanism of Action of Calcium Ionophores on Intact Cells: Ionophore-Resistant Cells. *Membrane Cell Biology* **2000**, *13(3)*, 357–368. PMID 10768486
10. Muñoz-Planillo, R. *et al.* K^+ Efflux is the Common Trigger of NLRP3 Inflammasome Activation by Bacterial Toxins and Particulate Matter. *Immunity* **2013**, *38(6)*, 1142–53. doi:10.1016/j.immuni.2013.05.016. PMID 23809161.

www.agilent.com/lifesciences/biotek

RA44186.321087963

Printed in the USA, February 1, 2021
5994-2572EN

Agilent
Trusted Answers